Journal of
Ship&Ocean
Technology
©MARCH 2007

SOTECH Vol. 11, No. 1, pp. 25 ~ 35, 2007

Fatigue Strength Assessment of TLP Tendon Porch Using API 2W Gr.50 Steel

Sung-Woo Im[1], Young-Seok Seo[2] and Joo-Sung Lee[2]

[1] Research Institute of Steel Technology, Giheung, Korea
[2] School of Naval Architecture & Ocean Engineering, University of Ulsan, Ulsan, Korea;
Corresponding Author: jslee2@mail.ulsan.ac.kr

Abstract

This paper is concerned with the fatigue strength assessment of tendon porch found which is categorized as the special structural member in TLP. Large-scale tendon porch specimens have been designed and fabricated with API 2W Gr.50 steel recently produced by POSCO. Fatigue test has been carried out for three tendon porch specimens under various load level. Fatigue strength has been evaluated based on the nominal stress range and the results are compared with the fatigue design curve of DnV RP-C203. From the present experimental study, it has been found that the porch specimens satisfy the fatigue design rule although test was carried out under the positive stress ratio. It can be, therefore, said that the API 2W steel produced by POSCO possess sufficient fatigue strength.
Keywords: fatigue damage ratio, fatigue strength, tendon porch, TLP, S-N curves, through-thickness crack

1 Introduction

TLP (tension leg platform) is well known as the appropriate offshore structure type for deep sea due to its excellent motion characteristics, flexibility in operation and so on. Among structural members, tendon porch at which tendons (tension leg) are attached is one of the most critical members because their failure must cause disaster of the whole TLP structure. Due to this reason tendon porch is categorized as the special category of structural member. Typical example of TLP is illustrated in Figure 1, which is the pontoon extension type. Tendon porch is subjected to varying load due to various sources such as wave, current, wind, motion and so on under the initial tension due to excessive buoyancy. Since tendon porch is easily expected to be subjected to varying load, fatigue failure is the most important failure mode, which should be, therefore, primarily taken into account at the design stage. According to the structural design rule of DnV OS-C105 tendon porch is made of API 2W steel as seen in Figure 2. POSCO has recently developed API 2W Grade 50 steel. As a new material is developed, the fundamental mechanical properties of the base metal and its weldments are evaluated as per test items in the API RP 2Z. However, this does not include the fatigue and brittle fracture of the base metal and its weldments of the structure fabricated with that material. In this regard it is very important to carry out a fatigue test to investigate the fatigue strength behavior when applied to the real structure.

The fatigue strength characteristics of API 2W Grade 50 steel developed by POSCO have been already evaluated by carrying out fatigue test with the large-scale tubular joint structure (Im et al 2005a, b) and the large-scale topsides joint structure (Im 2005).

In this study large-scale tendon porch models, that is 30% reduced model of the real tendon porch, were fabricated with API 2W Grade 50 steel and fatigue test were carried out under the various load level to evaluate the fatigue strength characteristics of the tendon porch structure as designed, base metal and weldments. Before conducting the present fatigue test, critical site where crack initiation was expected to start was anticipated from the results of structural analysis. The crack initiating position, crack propagation direction and fatigue life as the present test results are compared with those anticipated based on the result of structural analysis. It has been seen that the anticipated results showed good agreement with test results. Test results are also compared with the fatigue design curve of DnV RP-C203 and show the excellent fatigue strength characteristics.

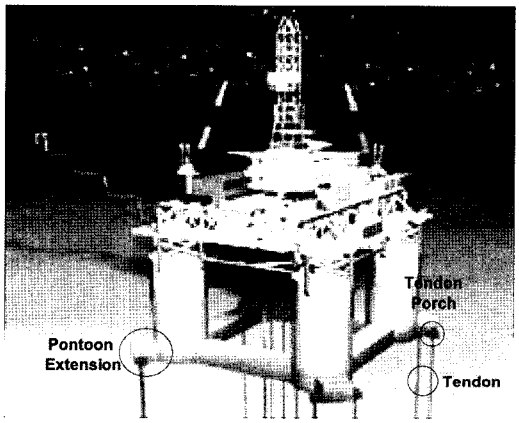

Figure 1: Example of TLP

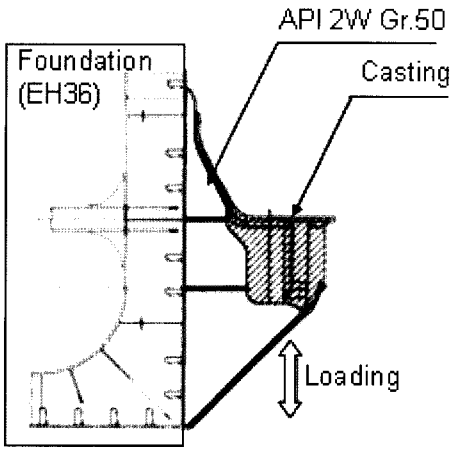

Figure 2: Steel grade used in tendon porch and loading

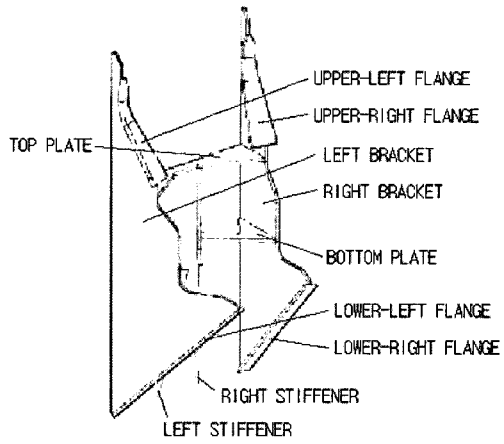

Figure 3: Structure of tendon porch for the present study

2 Structure design of tendon porch specimens

Tendon porch specimen was designed so as to represent the real model as accurate as possible. But geometric shape of some members was designed in the simple shape in order to reduce the inaccuracy in manufacturing. Since there is the possibility of buckling occurrence in bracket part under the loading in Figure 2, the bracket thickness is determined to prevent it (see terms of members in Figure 3). In addition although the thicknesses of members are different from member to member, all members of the present porch specimens are designed to be the same thickness except the casting part. Casting part is design to have sufficient thickness so as to behave as the rigid body. Finite element modeling of the present porch specimens is illustrated in Figure 4. Half of the whole structure is modeled due to symmetry in shape and loading. Shell elements are used for the present modeling. Fixed boundary conditions are imposed at the nodes attached to porch foundation and symmetric boundary conditions are imposed at nodes on the symmetry plane. Uniformly distributed load is imposed on the elements, which contact with loading jig.

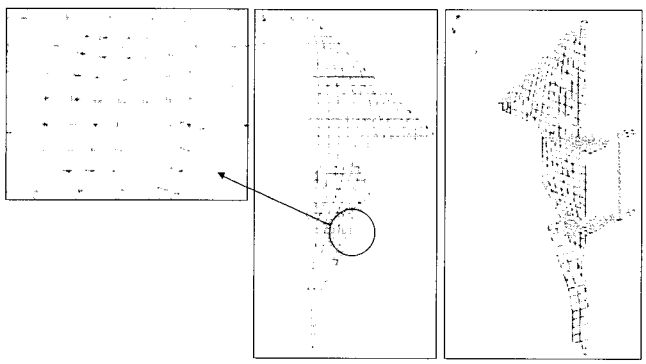

Figure 4: Finite element modeling of tendon porch

Stress distribution is illustrated in Figure 5 under the total load of 529.7 kN. As it can be expected, high stresses occur around the joint part of upper flange and casting part. Based

on the case study with varying thickness of members, their thickness were finally determined as 16mm considering the design condition that buckling should not occur at bracket part and the capacity of loading actuator which is to be used for the present fatigue test. In doing this fatigue strength is evaluated according to class D S-N curve of DnV RP-C203 (2001).

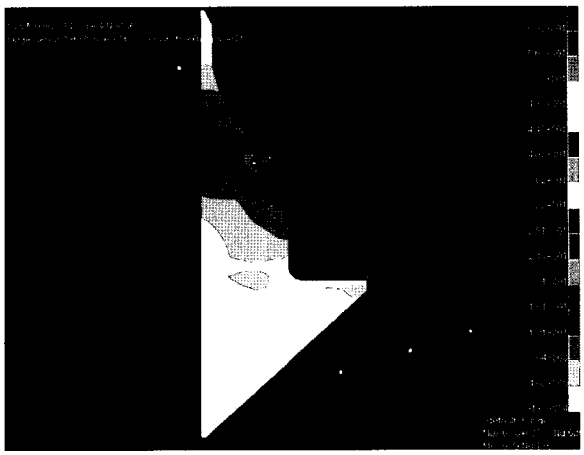

Figure 5: Stress distribution at bracket (major stress)

3 Manufacturing of tendon porch specimens

According to the structural design result in the last section, three specimens for the present fatigue test were fabricated as shown in Figure 6. Weld condition is summarized in Table 1. All welded parts are examined through ultrasonic test to check the welding defects. In Figure 6 the bottom plate is porch foundation, which is to be fixed on the floor during test. The member which is perpendicularly attached to the porch foundation is porch, the upper member of porch is casting, and the loading jig is attached on the casting part.

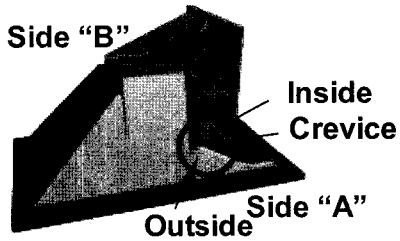

Figure 6: Shape of the present porch specimen

Table 1: Welding condition

Welding process	Welding consumable	Heat input (kJ/mm)	Interpass temp. (°C)	Polarity
FCAW	E81T1-K2	16.4	88	DCRP

4 Fatigue test

4.1 Specimen setting up and test scheme

Figure 7 shows the test specimen setting with loading frame and an actuator system. Porch foundation part in Figure 6 is fixed on the floor and casting part is connected with loading jig and 980 kN dynamic actuator. Static loads of various load level were applied before the fatigue test to remove the residual stresses due to welding. Since tendon is subjected to fluctuating load under the initial tensile state, sine wave load is applied with load ratio, R=0.1 to reflect such loading state. Frequency of loading was 5~6 Hz. Loading conditions for the three specimens which are designated as P1, P2 and P3, respectively are summarized in Table 2. Fracture is assumed when through thickness crack occurs.

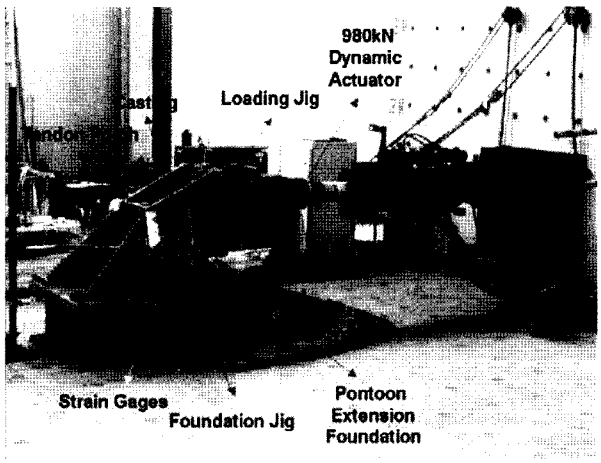

Figure 7: Test set up for specimen

Table 2: Loading conditions

Specimen	Load range, ΔQ	Road ratio
P1	1st: 441.5kN centre 2nd: 618.0kN 100mm up 3rd: 706.3kN 300mm up	0.1
P2	529.7kN 300mm up	0.1
P3	618.0kN 300mm up	0.1

4.2 Results of fatigue tests

(1) Specimen P1

Specimen P1 is loaded as three stages with varying load level while keeping the load ratio as R=0.1 until fracture occurs. Hereafter loading state is denoted as 'the minimum value / maximum values'. Loading history for the specimen P1 is as follows;

- 1st loading stage: Load 49.1/491.0kN was applied for 1,149,335 cycles.
- 2nd loading stage: Load 68.7/686.7kN for

1,112,873 cycles with moving loading jig upward by 100mm.

- 3rd loading stage: Load 78.5/784.8kN until fracture occurs with moving loading jig upward by 300mm.

Since load was eccentrically applied toward side A in Figure 6 during test, no cracks occurred at side B. Meanwhile, crack occurred at the connecting area of lower part of upper flange and bracket as it was expected from the structural analysis as shown in Figure 5 and propagated toward the inside of bracket. Fracture of P1 occurred at 227,596 cycles during the 3rd loading stage. Figure 8 shows the variation of stress of strain gages, which were attached around the critical location, that is, where crack initiated and propagated. In Figure 8 cycle when stress abruptly decreases corresponds to fracture time. The total number of cumulated cycles 2,489,804 until fracture occurred. The crack shape at the critical location is illustrated in Figure 9 with the stress distribution as the results of structure analysis. It can be seen that crack occurred at the expected location.

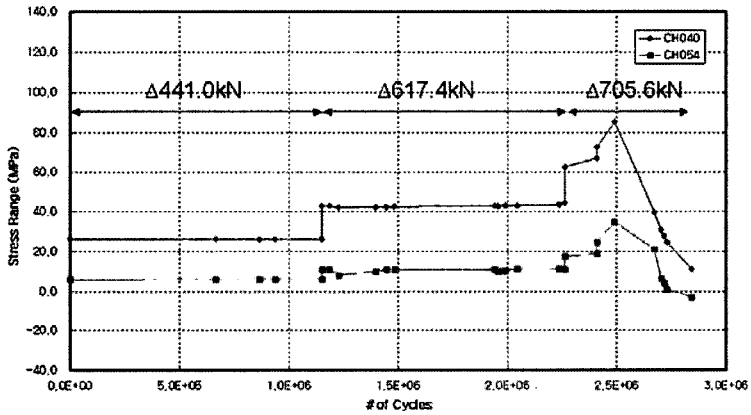

Figure 8: Variation of stress range to the cumulated loading cycle of specimen P1 (side A)

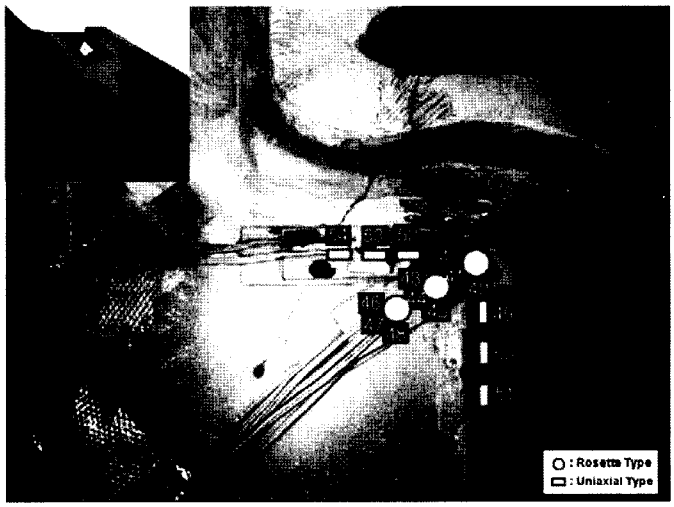

Figure 9: Crack at the critical location for specimen P1

(2) Specimen P2 and P3

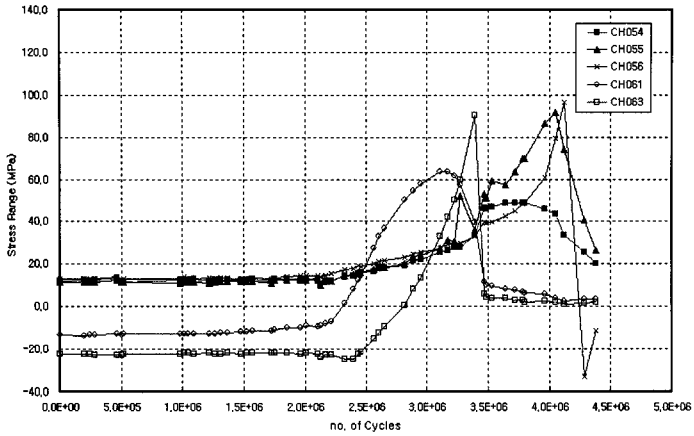

(a) side A

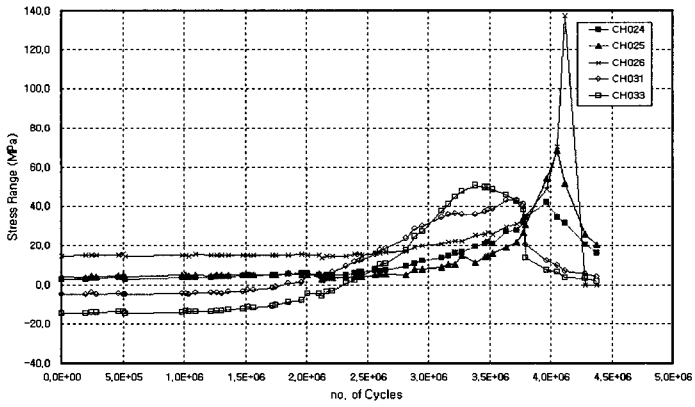

(b) side B

Figure 10: Variation of stress range to the cumulated loading cycle of specimen P2

Fatigue test was carried out for the specimen P2 and P3 with constant load range as shown in Table 2. Minimum/maximum load was 58.8/588.6kN and 68.7/686.7kN for specimen P2 and P3, respectively and load ratio R=0.1 was kept during test as before. Variation of stress range measured around the critical location to loading cycle is illustrated in Figure 10 for specimen P2. The strain gages #54, #55, #56, #61and #63 attached on side A are symmetrically correspond to the strain gages #24, #25, #26, #31 and #33 on side B as shown in Figure 11. As it can be seen in Figure 10, measured stress ranges are not completely symmetry due to the slight eccentricity of the applied load. But eccentricity seems to be smaller than the case of specimen P1. Similar stress variation was measured for specimen P3, which is not presented here.

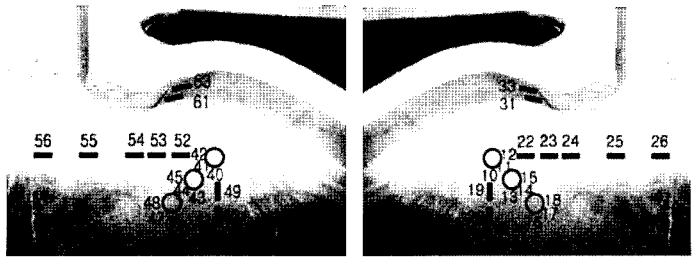

(a) side A (b) side B

Figure 11: Location of strain gages at the critical location

5 Comparison between results of test and analysis

In this section, the test results are firstly compared with the results of structural analysis in terms of the principal stresses. Stress components at the position where strain rosette can be calculated using the formulae between strains and stresses, which can be found in the most textbook for the mechanics of materials, for example see Pytel and Kiusalaas (2003). For the present test, 45 deg. strain rosettes were used to measure the strain components. Using such formulae three stress components, σ_x, σ_y and τ_{xy} for the plane stress state are to be obtained and then principal stresses and their directions can be easily calculated. To estimate the stress components with the structural analysis results at the same position where strain rosettes are attached, shape function of 4 node quadrilateral element is used. As it is well known, shape function used in finite element method is that relation function to relate any physical quantity and its nodal values (Cook et al. 2002). It can be therefore used to estimate stress components at any position in an element with the stress components at nodes.

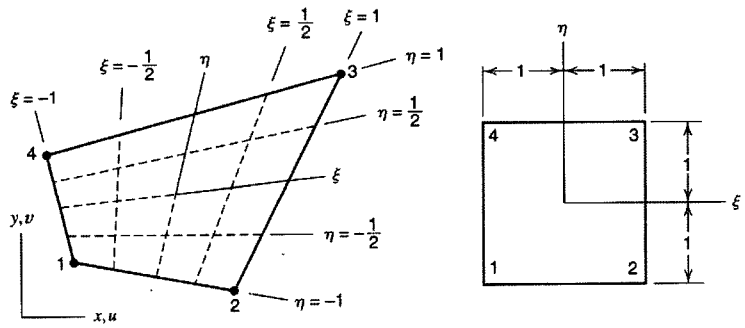

(a) in x-y coordinate system (b) in $\xi\eta$ coordinate system

Figure 12: Four node quadrilateral element

Shape functions of 4 node quadrilateral element (bi-linear element) in Figure 12 are given as follows.

$$\left.\begin{aligned} N_1 &= -\frac{1}{4}(1-\xi)(1-\eta)(\xi+\eta+1) \quad N_5 = \frac{1}{2}(1-\xi^2)(1-\eta) \\ N_2 &= +\frac{1}{4}(1+\xi)(1-\eta)(\xi-\eta-1) \quad N_6 = \frac{1}{2}(1+\xi)(1-\eta^2) \\ N_3 &= +\frac{1}{4}(1+\xi)(1+\eta)(\xi+\eta-1) \quad N_7 = \frac{1}{2}(1-\xi^2)(1+\eta) \\ N_4 &= -\frac{1}{4}(1-\xi)(1+\eta)(\xi-\eta+1) \quad N_8 = \frac{1}{2}(1-\xi)(1-\eta^2) \end{aligned}\right\} \tag{1}$$

where $\xi$and η are natural (or normalized) coordinates. The stress values at any position in an element $\sigma(x,y)$ is calculated as below.

$$\sigma(x,y) = \begin{bmatrix} N_1 & N_2 & N_3 & N_4 \end{bmatrix} \begin{Bmatrix} \sigma_1 \\ \sigma_2 \\ \sigma_3 \\ \sigma_4 \end{Bmatrix} \tag{2}$$

In eq.(2), $\sigma(x,y)$ is the stress at the given position x and y, which is to be calculated. σ_1, σ_2, σ_3, and σ_4 are stresses at four nodes in Figure 12, which can be σ_x, σ_y or τ_{xy}.

According to the method just described, stress components are calculated followed by the principal stresses and their direction. The comparison results are illustrated in Table 3 for the critical position and three strain gage position for specimen P1. In Table 3 θ_c is the crack propagation direction that is the direction of minimum principal stress. As it can be seen, good agreement is achieved between test and numerical analysis results.

Table 3: Comparison of principal stresses around the critical location and crack propagation direction for specimen P1

Position	Test result		Analysis result	
	Max. stress (MPa)	θ_c(°)	Max. stress (MPa)	θ_c(°)
critical location	-	about 33	68.6	40.3
gage #40~42	30.8	20.4	23.9	47.4
gage #43~45	27.0	31.6	27.8	55.0
gage #46~48	22.8	48.4	23.1	68.7

6 Fatigue strength evaluation of the present porch specimens

6.1 Specimen P1

Since specimen P1 was tested with three loading stage, direct comparison of fatigue strength with S-N curve is not easy. S-N fatigue damage approach under the assumption of linear cumulative damage is employed for the present study. Cumulative damage at each loading stage is summarized in Table 4 with stresses and cycles to failure. Since it would be reasonable to assume that crack initiated at weld toe, the stress at the weld toe is used in fatigue life calculation. In Table 4, stress at gage #40 is calculated with the measured strain and stress at weld toe is estimated by using Eq.(2) as described in the previous section.

Number of cycles for the 3rd loading stage is that minimum/maximum load of 78.5/784.8kN was applied till fracture occurred. Fatigue life on the 5th column is the calculated number of cycles with class D S-N curve of DnV RP-C203.

If the constant stress range of 139.3 MPa, which is the stress range at weld toe during the 3rd loading stage, is assumed to be applied from the 1st load, 0.540E+06 cycles is the theoretical fatigue life corresponding to this stress range. As the damage ratio cumulated up to the 3rd loading stage in the present test is 1.2194, the number of cycles according to this damage ratio is 0.658×10^6 cycles (=0.540×10^6 cycles x 1.2194). Therefore 0.658×10^6 cycles may be regarded as the number of cycles to failure when stress range of 139.3 MPa is assumed to be constantly applied from the 1st loading stage. This point is designated as ◆ (P1-A) in Figure 13.

Table 4: Cumulative damage at each loading stage for specimen P1

Loading stage	Stress at gage #40 (MPa)	Stress at weld toe (MPa)	No. of loading cycles ①	Fatigue life (class D) ②	Fatigue damage ratio Δ=①/②
stage 1:	26.2	55.6	1,149,335	7.32E+06	0.1366
stage 2:	42.8	95.4	1,112,873	1.68E+06	0.6621
stage 3:	62.5	139.3	227,596	0.54E+06	0.4217

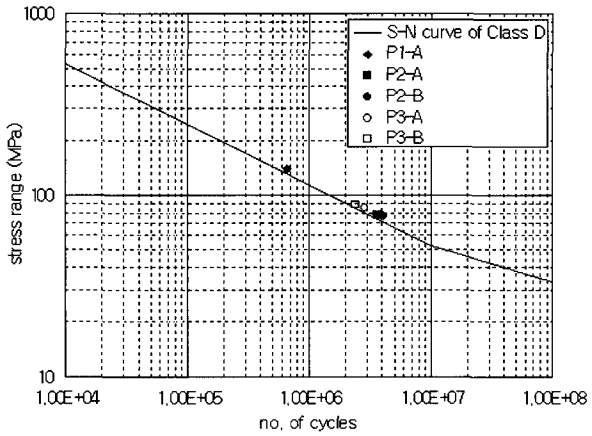

Figure 13: Comparison of the present fatigue test result with S-N Curve (class D)

6.2 Specimens P2 and P3

Constant load range was applied until fracture occurs for specimens P2 and P3, and their fatigue life can be directly compared with S-N curve. In Table 5, stress at weld toe estimated using Eq.(2) as before and no. of cycles at fracture in test are summarized with the theoretical fatigue lives calculated using S-N curve data of class D in DnV RP-C203. In all cases fatigue life of specimens is greater than the theoretically calculated one by about 16% at least. These results are also compared with S-N curve as shown in Figure 13. The points ■ (P2-A) and ● (P2-B) are corresponding to side A and B of specimen P2, and points ○ and □ to side A and B of specimen P3.

Table 5: Stress at weld toe and fatigue lives

Specimen		Stress at weld toe (MPa)	No. of cycles at fracture in test	Calculated fatigue life
P2	side A	78.2	3,639,197	3.051E+06
	side B	76.8	4,053,863	3.221E+06
P3	side A	84.7	2,861,911	2.401E+06
	side B	88.7	2,417,735	2.088E+06

As it can be seen in Figure 13, all points of the fatigue test for the present porch specimens lie above S-N curve. As mentioned before, the present test was carried out with load ratio, that is, stress ratio R=0.1. It is well known that fatigue life decreases when stress ratio is positive. Considering this fact it can be said that the API 2W Gr.50 steel produced by POSCO possess sufficient fatigue strength.

7 Conclusions

In this study, the fatigue test has been carried out for tendon porch which is categorized as the special structural member in TLP. Three specimens, which was designed as 30% reduced model of the real structure were fabricated with API 2W Gr. 50 steel of POSCO and fatigue test were carried out under the various load level. From the present experimental and numerical studies, it has been found that the porch specimens satisfy the fatigue design rule although test was carried out under the positive stress ratio. It can be, therefore, said that the API 2W steel recently produced by POSCO possess sufficient fatigue strength.

References

Im, S.W., I.H. Chang, K.K. Park, C.H. Jo and K.Y. Kim. 2005a. A Study on the Fatigue Crack in Large-Scale Tubular Joints for Offshore Structures, Proceedings of 5th ISOPE Conference, 341-345.

Im, S.W., I.H. Chang, C.H. Jo and K.K. Park. 2005b. Fatigue Behavior of Large Scale Tubular Joint for API 2W Gr.50 Steel, Journal of Ocean Engineering & Technology, **19, 3,** 54-58.

Im, S.W. 2005. A Prospective of Offshore Structure and Fatigue Tests of Large-Scale Structures, Proceedings of 14th Steel Usage Technology Conference, POSCO, 221-232.

Pytel, A. and J. Kiusalaas. 2003. Mechanics of Materials, Brooks/Cole-Thomson Learning, Inc.

Cook, R.D., D.S. Malkus, M.E. Plesha and R.J. Witt. 2002. Concepts and Applications of Finite Element Analysis, 4th edition, John Wiley & Sons, Inc.

DnV OS-C103. 2001. Structural Design of TLPs.

DnV RP-C203. 2001. Fatigue Strength Analysis of Offshore Steel Structures.